

# Automatic design of pixelated near-zero refractive index metamaterials based on elite-preserving genetic algorithm optimization

Shuo Sun, Yannan Jiang<sup>\*</sup>, Jiao Wang

School of Information and Communication, Guilin University of Electronic Technology, Guilin 541004, China

## ARTICLE INFO

### Keywords:

Near-zero refractive index metamaterial  
Pixelated metamaterial  
Genetic algorithm optimization  
Automatic design  
High directivity antenna

## ABSTRACT

Near-zero refractive index metamaterials (NZIM) have drawn a lot of attention recently for the development of high directivity antennas. However, their application has been constrained by the tedious and time-consuming manual design process. In this work, we offer an automated optimization design technique for NZIM that combines a modeling process based on pixelated metamaterials with an optimization process based on heuristic algorithms. The interactive CST-Python simulation is utilized for accomplishing the above automated design. In detail, the elite-preserving genetic algorithm (EGA) is specifically employed because of its improved capacity in locating the superior unit, and the fitness function proposed guarantees the performance of bandwidth and optimization process based on the principles of proportionate integration and penalty-like functions, respectively. Utilizing the suggested technique, we designed a NZIM unit that operates between 8.0 and 8.52 GHz. In order to validate the performance of the NZIM, a rectangular microstrip patch antenna (MPA) resonating at 8.2 GHz was employed as the radiation source for studies. According to the simulation results, the developed NZIM has a clearly beam focusing effect which causes the MPA's spherical waves to converge into quasi-plane waves. Furthermore, discussing the NZIM's application in high directivity antennas designing, the prototypes of the NZIM and MPA were fabricated and tested. The results revealed that the MPA's gain enhancement achieves 5.3 dB on average and 6.05 dB on maximum. Due to the automated optimization and design, this work is promised to advance NZIM's further applicability in high directivity antennas.

## Introduction

In the last decades, Metamaterials have undoubtedly been one of the hottest research topics in the field of electromagnetism. Owing to the controllable electromagnetic parameters (e.g. refractive index, dielectric constant, magnetic permeability, etc.), metamaterials achieve simple modulation of electromagnetic waves, which has led to a wide range of applications in the design of various microwave devices, e.g. polarization converters [1–3], absorbers [4–6], etc. Besides, it has shown great potential for optimizing the performance of conventional devices. Among them, a typical example is the near-zero refractive index metamaterials (NZIM) applied in the design of high directivity antennas [7–14]. Thanks to the beam convergence effect of NZIM, the significant gain enhancement are achieved when the NZIM are combined with the patch antennas [9–11], dipole antennas [12], and horn antennas [13]. Studying the NZIM's mechanism from a microscopic perspective, its electromagnetic parameters are actually equal to the resonant characteristics carried by the units that make it up. Therefore, the design of the

resonant structure of the unit has become the main direction of NZIM research. In earlier reports, conventional structures include single-slit ELCs [7], crosses [9], open resonant rings [10], etc., and most of the later studies follow or improve such structures. Unfortunately, metamaterial design based on the above strategies relies heavily on physical insight, expert experience and trial-and-error optimization, which significantly constrains design efficiency. Fortunately, with the rapid development of artificial intelligence, heuristic algorithms such as genetic algorithms (GA) [15–18] and particle swarm algorithms [19,20] are widely applied in the optimization of electromagnetic designs. In particular, it has been proven that GA offers substantial advantages in simplifying the metamaterial optimization by replacing the manual parameters scanning. This is due to the robust global search capabilities and various operators. However, these optimization techniques are still intended for a sample to be improved, and further investigation into improved performance is restricted by the minor changes brought about by modifications to the regular pattern's resonant structure. Later, it was reported by H. Chen's study [21] that metamaterials with unintentional

\* Corresponding author.

E-mail address: [ynjiang@guet.edu.cn](mailto:ynjiang@guet.edu.cn) (Y. Jiang).

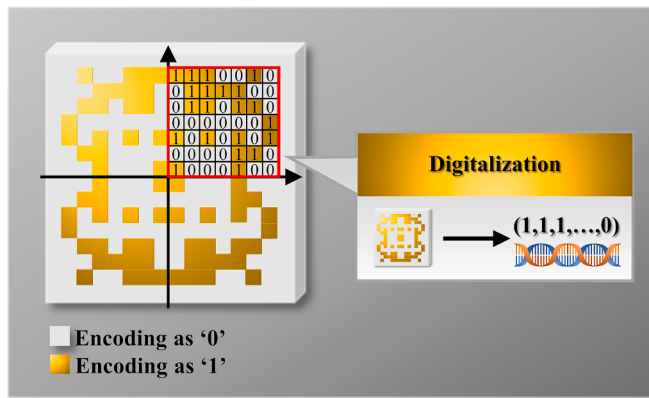


**Fig. 1.** The process of pixelated metamaterial modeling.

irregular patterns such as maps and reliefs also exhibit surprising excellent electromagnetic properties in certain frequency bands. Although the complex structure of these metamaterials was difficult to design and their electromagnetic parameters are not controllable at that time, it enlightens new ideas for investigating the performance enhancement of metamaterials. It's exciting to note that the design process for pixelated metamaterials, which has been reported in recent research [22–25], has provided fresh insight into the modeling of complicated and atypical resonant structures. In this method, the resonant structure on the unit surface is discretized into  $n \times n$  pixel lattices and coded as "1" and "0" according to whether the lattice is covered with metal patches or not, respectively. Thus, a complicated geometric model is converted to a binary sequence, enabling the artificial construction of more intricate and varied resonant structures. Further, an optimization algorithm is applied to reorganize and optimize the binary sequence to

obtain a unit that meets the design requirements. Utilizing this method, a study by Tung, L.V. et al., in 2020 [26] implemented the design of an NZIM. Its optimization was carried out using a classical genetic algorithm (CGA). The designed near-zero refractive index metamaterial loaded onto a rectangular microstrip patch antenna (MPA) achieved a gain enhancement of 3.75 dB. However, the CGA utilized has inherent flaws that make it challenging to maintain superior genetics, leading to poor performance finding. Furthermore, the fitness function utilized in the design disregards bandwidth, which has an impact on the usefulness of the constructed NZIM.

This study proposes an automated optimization design technique for NZIM which was inspired by reports on pixelated metamaterials. It is built on joint Python-CST automated simulation and optimization by an elite-preserving genetic algorithm (EGA). The weaknesses of the prior study are addressed with corresponding enhancements. Firstly, the EGA, which has a better search capability, is utilized as the optimization algorithm in the design. In addition, the fitness function based on proportional integration and penalty-like functions is proposed to fulfill the bandwidth metrics and to further improve the convergence speed of the algorithm. The flow of the design method is as follows. Firstly, the resonant structure of the unit to be designed is discretized into a  $14 \times 14$  pixel lattices which is characterized numerically using a binary sequence code, and a randomly generated sequence is employed to generate the initial population. Next, EGA is applied to optimize the initial population. Finally, the designed NZIM unit is obtained after 30 generations of evolution and achieves near-zero refractive index ( $n_{re} < 1$ ) in the range of 8.0–8.52 GHz. To validate the performance of the designed NZIM, a rectangular microstrip patch antenna (MPA) resonating at 8.2 GHz was utilized as the radiation source for the experiments. The near-field simulation results show that the NZIM has a significant beam-shaping effect where the spherical wave radiated by the MPA becomes a quasi-plane wave after passing through the NZIM. To further investigate the

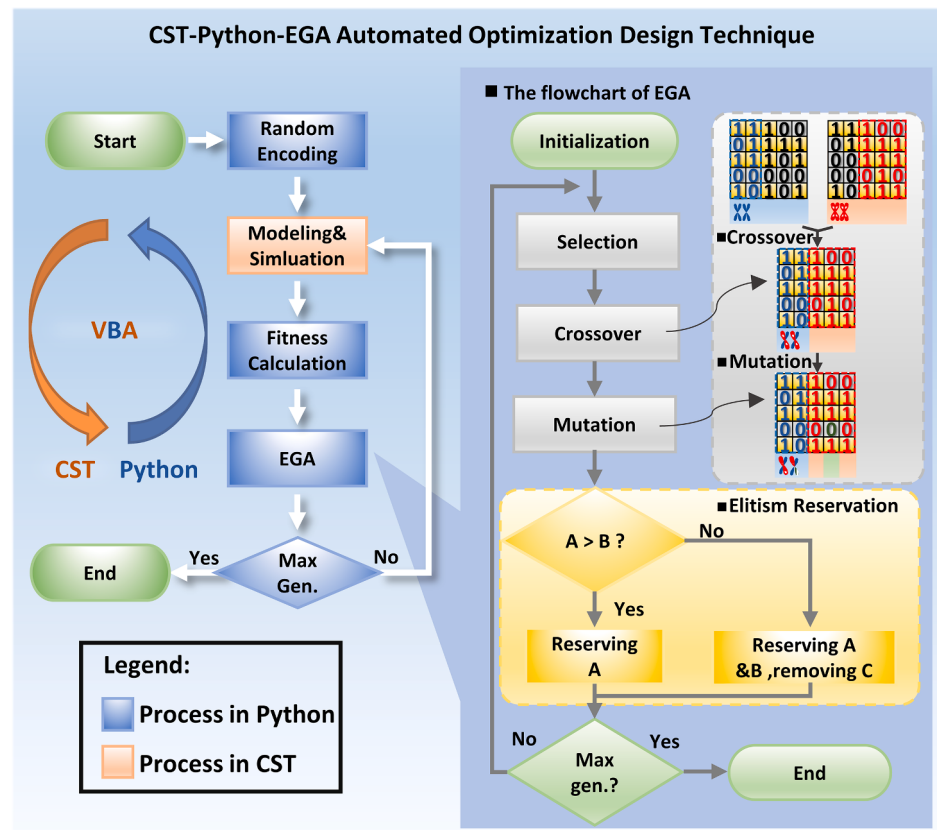


**Fig. 2.** The flowchart of the automated optimization design technique and EGA.

application of the designed NZIM in the directionality enhancement of the antenna, we manufactured the prototypes of NZIM and MPA. Then, the radiation characteristic of the prototypes is measured in the near-field test system. The measured results demonstrated that the directionality of the antenna was greatly improved after loading the NZIM, with an average gain improvement and a maximum gain improvement of 5.3 dB and 6.05 dB respectively.

This paper is organized as follows. In the section II, the design method and the designed metamaterial unit are presented. In section III, the simulation and test results are discussed.

## Design technique

### *Pixelated metamaterial modeling*

Based on the pixelated metamaterial modelling technique, the resonant structure of the unit surface is divided into  $14 \times 14$  pixel lattices and the complex model is digitized into a binary sequence by coding, as shown in Fig. 1. The pixel lattices are coded as "1" and "0" depending on whether they are covered with metal patches or not. In addition, a single quadrant symmetry was used to simplify the coding length, reducing it to 1/4 of the original.

### *CST-Python-EGA automated optimization simulation design*

Despite the fact that the pixelated metamaterials modeling technique makes it accessible to design units with more complicated resonant structures, the sequences arising from the numerous pixel lattices that comprise these units are still quite challenging for manual simulation. Here, we offer a CST-Python-EGA based automated design technique to address this issue. Through the built-in VBA interface of CST, Python is utilized in the setup of modeling and simulation. Additionally, the evolutionary process that EGA simulates allows for automated iterative optimization of the model. Fig. 2 depicts the design method's flowchart. The simulation process begins with the generation of the initial model characterized by a random binary sequence. Next, the modeling and simulation process sequencing complete in CST. Then, the simulation results are fed into Python for the extraction of electromagnetic parameters and the calculation of fitness to evaluate the performance and begin the EGA optimization process. Finally, if the maximum number of iterations is satisfied, the simulation will either come to a conclusion or go on.

### *EGA design*

Classical genetic algorithm is an optimization algorithm proposed by Holland in 1975[27] inspired by natural selection. It utilizes the fitness function to evaluate the individuals among them, and achieves superiority by the strategy of making individuals with higher fitness (better performance) have a higher probability of entering the genetic process. The operators are employed to simulate the process of the selection, crossover and mutation in the biological genetic process. However, the CGA reveals deficiencies in solving certain optimal value problems, which fails to achieve convergence. Rudolph demonstrated this issue using finite Markov chain theory in his related work [28]. The reason for this is that superior genes are destroyed by the straightforward crossover operator employed by traditional genetic algorithms, making it challenging to maintain good genes. To solve this problem, EGA was created [29], which preserves the genetic process of CGA and replicates the individuals with the highest fitness in the current population directly to the next generation by skipping the genetic process. In this work, we applied EGA to the optimization, and its flowchart is depicted in Fig. 2. In which, the selection procedure uses a roulette wheel operator, which chooses candidates based on how fit they are relative to the population as a whole. i.e., the greater the percentage of individuals, the greater the likelihood of getting chosen. The single-point crossover operator is used

in the crossover process, which finishes the selection by randomly choosing the crossover point on the binary sequence and switching the chromosomes on the same side or on the opposite side with an equal chance of doing so. In order to visually illustrate the evolution of the NZIM unit in EGA, the process of crossover and mutation is also described specifically in Fig. 2. Then, the step of elite retention carries out, first, the generated individuals are sorted by fitness value and the top 20% are selected as elites. After that, the elite individuals in this generation (denoted by A in Fig. 2) are compared with the elite individuals of the current entire population (denoted by B in Fig. 2), and if the fitness of the elite individuals in this generation is greater than that of the elite individuals of the current entire population, the elite individuals of the population are replaced. Conversely, the elite individuals of this generation are retained and the worst adapted individuals of this generation are removed (denoted by C in Fig. 2). Additionally, the maximum genetic generation was set at 30 generations, and the population size was set at 30 individuals each generation.

### *Fitness function design*

In automated optimum design, in the same manner that the performance of a created NZIM is directly evaluated based on the value of the refractive index in human design, the computer often needs a function to evaluate the performance evaluation, i.e., the fitness function. For future optimization, the fitness function selection is essential and may affect both the rate of convergence and the outcome. In a related work [26] from 2020, Tung, L.V. et al., developed a fitness function represented by Eq. (1).

$$F = |\varepsilon_{re}(f)| + |\mu_{re}(f)| \quad (1)$$

where  $\varepsilon_{re}(f)$  and  $\mu_{re}(f)$  represent the relative permittivity and relative permeability at the frequency characterized by  $f$ , respectively, and  $F$  denotes the fitness. The equation is based on the relative refractive index equation  $n_{re} = \sqrt{\varepsilon_{re}\mu_{re}}$  and a near-zero refractive index ( $|n_{re}| < 1$ ) is obtained when the sum of  $\varepsilon_{re}$  and  $\mu_{re}$  amplitudes approaches zero. However, the issue of invalid -optimal solutions in the optimization process can arise with this equation. For example, even with a bandwidth of only 10 MHz, a unit with a  $n_{re}$  extremely close to zero at the point  $f$ , will be considered as the optimal solution and further output. Obviously, it is challenging to use NZIM units with such incredibly small bandwidths in real-world applications.

Here, as demonstrated in Eq. (2–4), we offer a fitness function design that accounts for the NZIM bandwidth to address this issue. In Eq. (2), the sampling ratio is utilized to reflect the

$$num = \frac{count(|n_{re}(f_i)|)}{N} \quad (2)$$

$$n_{am} = \sum_{i=N_1}^{N_2} \Delta f \cdot |1 - n_{re}(f_i)| \quad (3)$$

$$Fitness = \begin{cases} num + n_{am} & num > 0 \\ 0.001 & num = 0 \end{cases} \quad (4)$$

unit. The higher the proportion of sampling points satisfying the  $n_{re}$  near zero to the total sampling points (denoted by  $N$ ) indicates that the NZIM has a wider operating bandwidth. In Eq. (3), based on the proportional integration, the  $n_{re}$  of the unit is reflected in the form of the area of the curve. The NZIM has a refractive index closer to zero if the region enclosed by the refractive index curve and the straight line with  $n_{re} = 1$  is higher. Where  $\Delta f$  represents the sampling interval,  $n_{re}(f)$  represents the relative refractive index at the sampling point, and  $N_1-N_2$  represent the range of  $n_{re}$  near zero. As shown in Eq. (4), this is the fitness function used in this design. Here, considering the design requirement as a multi-objective optimization problem that satisfies both bandwidth and near-zero objectives, the two optimization objectives are weighted, with each

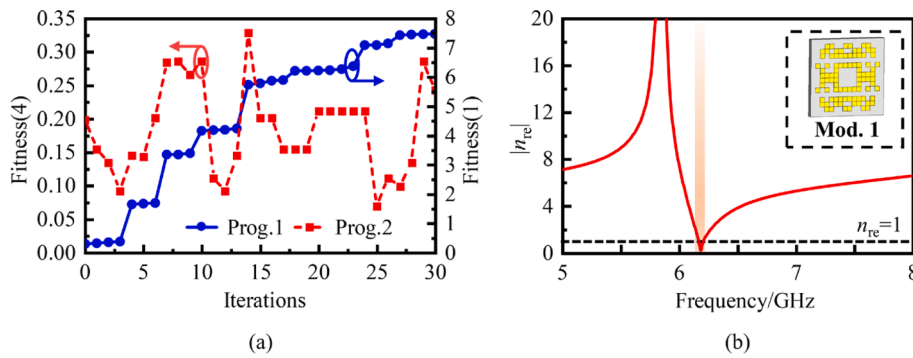


**Fig. 3.** (a)Fitness function performance comparison, (b)the  $n_{re}$  of Mod. 1.

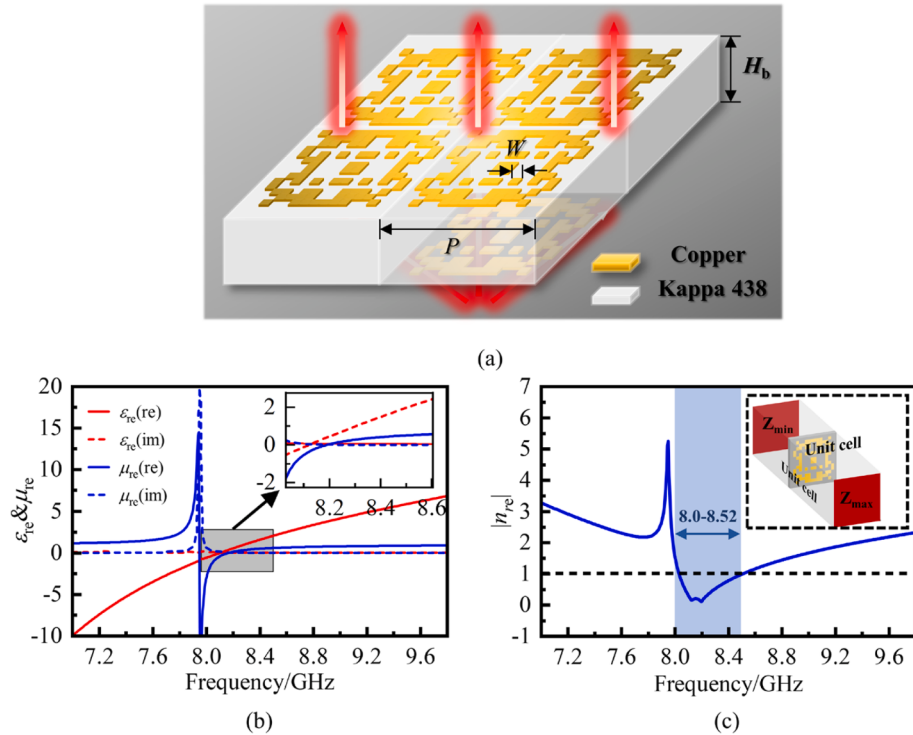


**Fig. 4.** (a)The designed NZIM unit, (b) equivalent relative permittivity and permeability, and (c) equivalent refractive index and the boundary conditions.

objective occupying the same weight. In particular, in order to reduce the risk of falling into a local optimum in the late stage of population evolution due to a single genotype, the fitness value of the  $num = 0$  unit is added to enrich the genetic diversity of the population during the evolution, based on the setting of the “penalty function”. To further illustrate the outstanding effect of the designed fitness function, the fitness function shown in Eq. (1) (i.e., Prog. 1) and the fitness function shown in Eq. (4) (i.e., Prog. 2) are used for optimization, and the results are compared in Fig. 3(a). It can be clearly seen that Prog.1 does not achieve a stable optimization search process compared to Prog.2. And Fig. 3(b) displays the  $n_{re}$  of the best fitness model (Mod. 1) that was produced in Prog. 1. In which, the minimum  $n_{re}$  is merely 0.2, but the bandwidth is only 40 MHz, which corresponds to the defect of the invalid -optimal solution in the previous section.

#### Designed NZIM unit

The NZIM unit designed by the proposed automated optimization design technique is presented in Fig. 4(a). In which, the metallic resonant structures consisting of  $14 \times 14$  arranged pixel lattices with side

length  $W = 1$  are etched on both sides of a Kappa 438 substrate with the thickness of  $H_b = 1.524$  mm. The relative permittivity of the substrate is 4.38 and the loss angle tangent is 0.005. The period of the unit  $P = 15.2$  mm, which is a slightly larger than the length of the sides of the resonant structure, is used to lessen coupling between the resonant structures of adjacent units. During the automated optimization simulation mentioned in the previous paragraph, the unit electromagnetic parameters were calculated, and the results are presented in Fig. 4(b) and (c), respectively. Among them, the electromagnetic parameters are extracted by the inversion algorithm based on the K-K relationship[30] and the boundary conditions are specified in the CST as shown in Fig. 4. (c). It can be seen that  $\epsilon_{re}$  and  $\mu_{re}$  are very close to zero at around 8.2 GHz, which contributes the  $n_{re}$  with an amplitude of merely 0.04 at that point, and the  $n_{re}$  is near zero in the frequency from 8.0 to 8.52 GHz.

#### Simulation & measurement

Due to validate the performance of the designed NZIM, a MPA resonating at 8.2 GHz is utilized here as a radiation source for study, as shown in Fig. 5(a). It is fabricated from a 1.5 mm thick F4BM-2 substrate

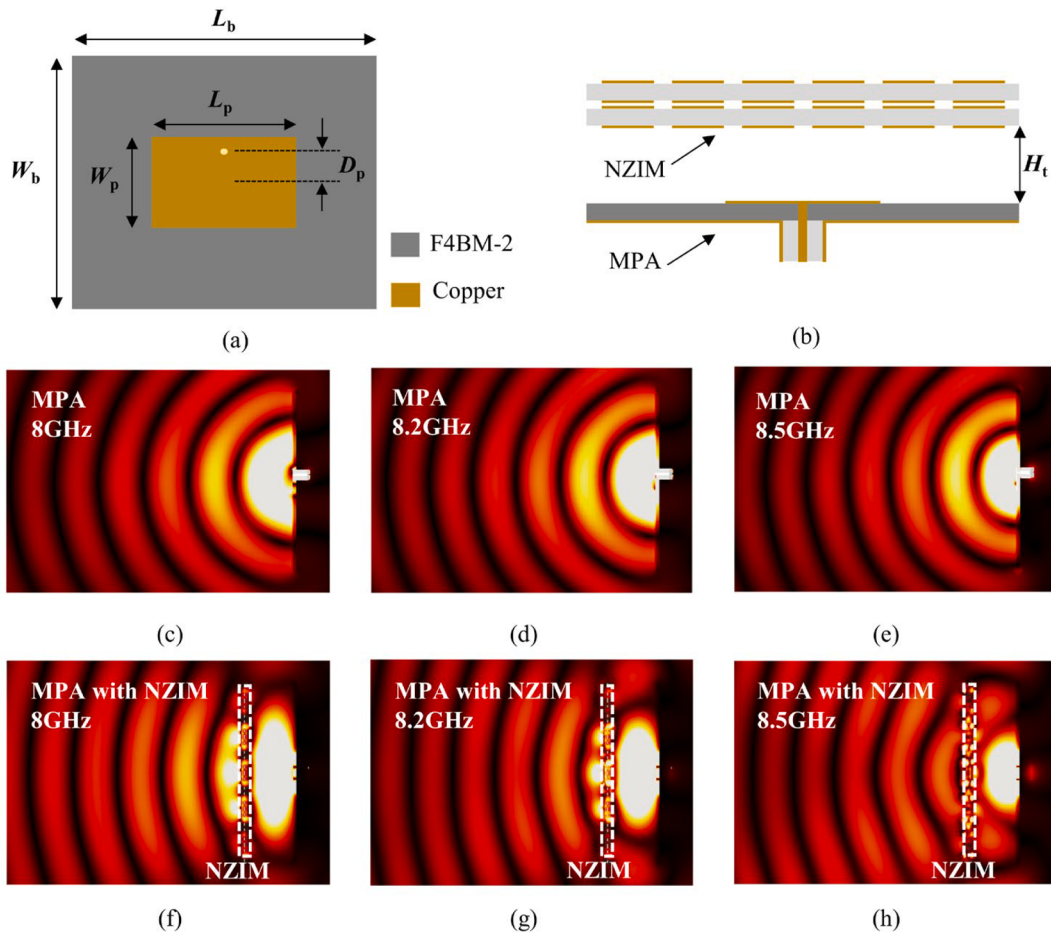


**Fig. 5.** The fabricated prototypes of MPA and NZIM cladding. (a) Top view of MPA and its geometrical parameters (mm) with  $L_b = 76$ ,  $W_b = 76$ ,  $W_p = 9.9$ ,  $L_p = 13.5$ ,  $D_p = 2.8$ , and  $H_t = 19.2$ , (b) side view of MPA, (c, d&e) the electric field of MPA at 8 GHz, 8.2 GHz, and 8.5 GHz, (f, g&h) the electric field of MPA with NZIM at 8 GHz, 8.2 GHz, and 8.5 GHz.

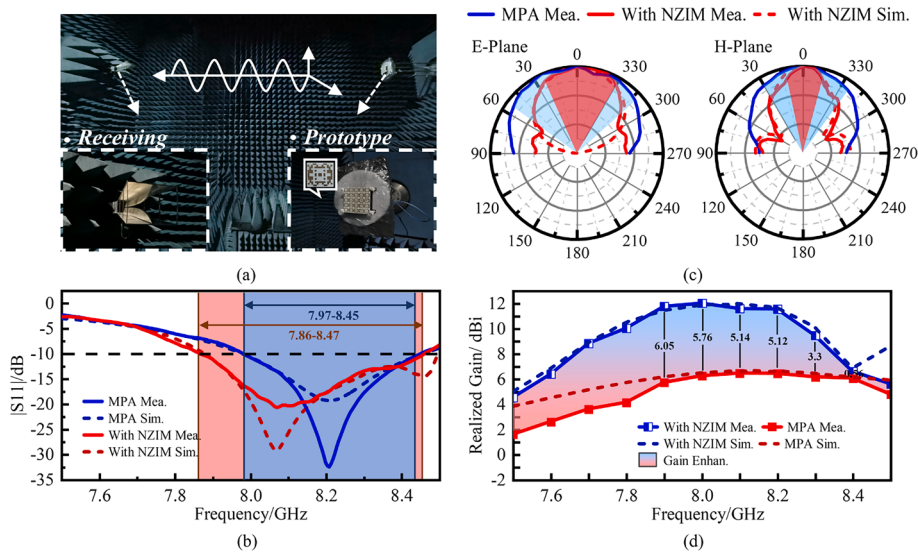


**Fig. 6.** Experimental environment and data. (a) Near-field test system, (b) S11, (c) radiation patterns at 5.8 GHz, and (d) gains.

with a relative permittivity equal to 2.65 and a loss angle tangent equal to 0.002. Further, a  $5 \times 5$  arrangement of NZIM units are loaded above the MPA, as depicted in Fig. 5 (b). Here, two layers of NZIM are utilized as a cladding layer to extend the propagation path of electromagnetic

waves in NZIM, which highlight the effect with NZIM in this way. The distance between the cladding layer and the MPA,  $H_t = 19.2$  mm, is about  $\lambda_0/2$ . (8.2 GHz corresponding to the wavelength). The distribution of the electric field in the CST was observed before and after the

**Table 1**

Comparison of this work with the other reports.

Ref.	Center frequency	Gain enhancement	Design method
8	6 GHz	1 dB	Manual
9	43 GHz	5 dB	Manual
14	6 GHz	3 dB	Manual
26	5.8 GHz	3.75 dB	Auto
This	8.2 GHz	6.05 dB	Auto

radiation source was loaded with NZIM, as depicted in Fig. 5(c-e) and (f-h), respectively. It is evident that the spherical waves radiated by the MPA are shaped into quasi-plane waves after passing through the cladding in the near-zero frequency band of the metamaterial. Its indicates that the designed NZIM has outstanding beam shaping effect.

It is also detailed how the developed NZIM may be used to create high directivity antennas. Here, as seen in Fig. 6(a), the NZIM cladding and MPA prototypes are processed for testing.

Additionally, the vector network analyzer (AV3656B) and near-field measuring equipment (see Fig. 6(a)) were used to examine the reflection coefficient and radiation properties. The reflection coefficient observed is displayed in Fig. 6(b), where it can be seen that the measurement is in agreement with the simulation and has only a little effect on the bandwidth of MPA after loading NZIM. After loading NZIM, the bandwidth ranges from 7.86 GHz to 8.47 GHz, covering the original MPA's bandwidth range of 8 GHz to 8.45 GHz. However, the impedance shift brought by the cladding makes it somewhat broader than MPA. In Fig. 6(c), the radiation direction patterns measured at 8.2 GHz is presented. It can be clearly observed that the half-power beam width is significantly narrower after loading the cladding, with a reduction of 23.6° and 83.9° in the E-plane and H-plane, respectively. This indicates that the directivity of the MPA is greatly improved thanks to the quasi-plane wave after loading the NZIM shown in Fig. 5. At the same time, the gain measured reveals a more intuitive elaboration, as we can see in Fig. 6(d). The gain of MPA is significantly improved after loading NZIM, with an average gain of 5.3 dB and a maximum gain of 6.05 dB.

Table 1 compares the reported works on NZIM for high directivity antenna applications with the performance comparison, where literature [8,9,14] is the manual design technique and literature [26] is an automated design that is similar to the manual design. It is obvious that the NZIM suggested in this article has a stronger gain-enhancing impact.

## Conclusion

In conclusion, we present an automated optimization design technique for NZIM, which is based on the modeling process of pixelated metamaterials and the optimization process of elite-preserving genetic algorithms, implemented by joint simulation of CST and Python. Applying the proposed method, we designed a NZIM unit operating at around 8.2 GHz. To verify its performance, it was loaded over a MPA resonating at 8.2 GHz for simulation and prototype testing. The test results show that the developed NZIM has a significant beam focusing effect, and its loading onto the MPA achieves a significant gain improvement of 5.3 dB on average and 6.05 dB on maximum. It is promised to promote the further application of NZIM in the design of highly directional antennas.

## Data availability

The data that support the findings of this study are available from the corresponding author upon reasonable request.

## CRediT authorship contribution statement

**Shuo Sun:** Conceptualization, Methodology, Writing – original draft, Visualization, Data curation, Formal analysis. **Yannan Jiang:** Project

administration, Funding acquisition, Supervision, Investigation, Writing – review & editing. **Jiao Wang:** Investigation, Writing – review & editing, Validation.

## Declaration of Competing Interest

The authors declare that they have no known competing financial interests or personal relationships that could have appeared to influence the work reported in this paper.

## Data availability

Data will be made available on request.

## Acknowledgement

The authors would like to acknowledge the National Natural Science Foundation of China (62261015), Natural Science Foundation of Guangxi Province (2019GXNSFFA245002), Key Laboratories for National Defense Science and Technology (202003007), and Guangxi Key Laboratory of Wireless Wideband Communication and Signal Processing (GXKL06190118) for their support of this work.

## References

- [1] Li F, Chen H, Zhang L, Zhou Y, Xie J, Deng L, et al. Compact high-efficiency broadband metamaterial polarizing reflector at microwave frequencies. *IEEE Trans Microw Theory Tech* 2018;1–9.
- [2] Zhu L, Zhao X, Miao FJ, Ghosh BK, Dong L, Tao BR, et al. Dual-band polarization converter based on electromagnetically induced transparency (EIT) effect in all-dielectric metamaterial. *Opt Express* 2019;27.
- [3] Xu ST, Fan F, Chen M, Ji YY, Chang SJ. Terahertz polarization mode conversion in compound metasurface. *Appl Phys Lett* 2017;111:031107.
- [4] Min P, Song Z, Yang L, Dai B, Zhu J. Transparent ultrawideband absorber based on simple patterned resistive metasurface with three resonant modes. *Opt Express* 2020;28.
- [5] Yazdi M, Albooyeh M, Alaei R, Asadchy V, Komjani N, Rockstuhl C, et al. A bianisotropic metasurface with resonant asymmetric absorption. *IEEE Trans Antennas Propag* 2015;63:3004–15.
- [6] Zhu Y, Long H, Liu C, Zhang H, Cheng Y, Liu X. An ultra-thin ventilated metasurface with extreme asymmetric absorption. *Appl Phys Lett* 2022;120:141701.
- [7] Bakhtiari A. Investigation of enhanced gain miniaturized patch antenna using near zero index metamaterial structure characteristics. *IETE J Res* 2022;68:1312–9.
- [8] Boubakri A, Choubeni F, Vuong TH, David J. A near zero refractive index metalens to focus electromagnetic waves with phase compensation metasurface. *Opt Mater* 2017;69:432–6.
- [9] Bouzouad M, Chaker S, Bensafielddine D, Laamari E. Gain enhancement with near-zero-index metamaterial superstrate. *Appl Phys A* 2015;121:1075–80.
- [10] Mri A, Mti A, Mm A, Ms B, Bb A, Ha C, et al. Square enclosed circle split ring resonator enabled epsilon negative (ENG) near zero index (NZI) metamaterial for gain enhancement of multiband satellite and radar antenna applications - ScienceDirect. *Results Phys* 2020;19.
- [11] Singh AK, Abegaonkar MP, Koul SK. High-gain and high-aperture-efficiency cavity resonator antenna using metamaterial superstrate. *IEEE Antennas Wirel Propag Lett* 2017;1–1.
- [12] Turpin JP, Wu Q, Werner DH, Martin B, Bray M, Lier E. Near-zero-index metamaterial lens combined with AMC metasurface for high-directivity low-profile antennas. *IEEE Trans Antennas Propag* 2014;62:1928–36.
- [13] Wu Q, Pan P, Meng F-Y, Li L-W, Wu J. A novel flat lens horn antenna designed based on zero refraction principle of metamaterials. *Appl Phys A* 2007;87:151–6.
- [14] Dawar P, Abdalla MA. Near-zero-refractive-index metasurface antenna with bandwidth, directivity and front-to-back radiation ratio enhancement. *Journal of Electromagnetic Waves and Applications* 2021;35:1863–81.
- [15] Ares-Pena FJ, Rodriguez-Gonzalez JA, Villanueva-Lopez E, Rengarajan S. Genetic algorithms in the design and optimization of antenna array patterns. *IEEE Trans Antennas Propag* 1999;47:506–10.
- [16] Clemens S, Iskander MF, Yun Z, Rayno J. Hybrid genetic programming for the development of metamaterials designs with improved characteristics. *IEEE Antennas Wirel Propag Lett* 2018;17:513–6.
- [17] Rayno J, Iskander M, Kobayashi M. Hybrid genetic programming with accelerating genetic algorithm optimizer for 3D metamaterial design. *IEEE Antennas Wirel Propag Lett* 2016;1–1.
- [18] Smith JS, Baginski ME. Thin-wire antenna design using a novel branching scheme and genetic algorithm optimization. *IEEE Trans Antennas Propag* 2019;67:2934–41.
- [19] Jia X, Lu G. A hybrid Taguchi binary particle swarm optimization for antenna designs. *IEEE Antennas Wirel Propag Lett* 2019;18:1581–5.

- [20] Jin N, Rahmat-Samii Y. Parallel particle swarm optimization and finite-difference time-domain (PSO/FDTD) algorithm for multiband and wide-band patch antenna designs. *IEEE Trans Antennas Propag* 2005;53:3459–68.
- [21] Chen H, Ran L, Wang D, Huangfu J, Jiang Q, Kong JA. Metamaterial with randomized patterns for negative refraction of electromagnetic waves. *Appl Phys Lett* 2006;88:031908.
- [22] Ranjan P, Mahato SK, Choube A, Sinha R, Peraza-Vázquez H, Barde C, et al. The synthesis of a pixelated metamaterial cross-polarizer using the binary wind-driven optimization algorithm. *J Comput Electron* 2022;21:453–70.
- [23] Luo P, Lan G, Nong J, Zhang X, Xu T, Wei W. Broadband coherent perfect absorption employing an inverse-designed metasurface via genetic algorithm. *Opt Express* 2022;30:34429–40.
- [24] Sui S, Ma H, Wang J, Feng M, Pang Y, Zhang J, et al. Synthetic design for a microwave absorber and antireflection to achieve wideband scattering reduction. *J Phys D Appl Phys* 2018;52:035103.
- [25] Zhang Q, Wan X, Liu S, Yin JY, Zhang L, Cui TJ. Shaping electromagnetic waves using software-automatically-designed metasurfaces. *Sci Rep* 2017;7:3588.
- [26] Tung LV, Ha-Van N, Seo C. A novel metamaterial design using genetic Algorithm for high gain energy harvesting antenna. In: in 2020 IEEE Wireless Power Transfer Conference (WPTC); 2020. p. 123–6.
- [27] Holland, “Adaptation in natural and artificial systems : an introductory analysis with application to biology,” *Control & Artificial Intelligence* (1975).
- [28] Rudolph G. Convergence analysis of canonical genetic algorithms. *IEEE Trans Neural Netw* 1994;5:96.
- [29] Bhandari D, Murthy C, Pal SK. Genetic algorithm with elitist model and its convergence. *Int J Pattern Recognit Artif Intell* 1996;10:731–47.
- [30] Szabo Z, Park G-H, Hedge R, Li E-P. A unique extraction of metamaterial parameters based on Kramers-Kronig relationship. *IEEE Trans Microw Theory Tech* 2010;58:2646–53.